GEOFIZIKA	Vol. 4	1987

Conference paper
UDC 551.465, 551.553

Air–sea interaction in the vicinity of the land–sea boundary in the presence of upwelling*

Borivoj Rajković and George L. Mellor***

** Faculty of Natural and Mathematical Sciences*
Dept. of Physics and Meteorology
P.O.B. 550 Belgrade,
Yugoslavia

*** GFD Program*
Princeton University
Princeton, N.J. 08540
USA

In order to examine a possible sea–air interaction in the vicinity of the western edges of continents, successive integrations of a 2-D atmosphere and ocean models were performed. The ocean model had prescribed wind forcing that was obtained from the atmosphere model which in turn had prescribed sea surface temperature resembling one for well developed upwelling.

Both models are for a hydrostatic and Boussinesq fluid with a sigma coordinate system. They have high resolution in the horizontal and a very high resolution in the vertical, capable of resolving both top and bottom boundary layers. Turbulent fluxes and mixing coefficients are parameterized with the so-called 2.5 level, second order closure scheme proposed by Mellor and Yamada. Seaward boundary conditions for the ocean model and lateral boundary conditions for the atmosphere model were of the radiation type. The ocean model had prescribed sea surface elevation and y-component of the pressure (buoyancy) field from the available data.

The diurnal cycle for the atmosphere model was implemented through the specification of the land surface temperature while night time cooling was modeled with a Newtonian forcing. The reference thermodynamic state of the atmosphere model was very similar to the observed state of the atmosphere in the Coastal Ocean Dynamics Experiment while enviromental winds were specified to give values for the wind-stress close to the observed climatological values.

The significant modification of the wind-stress profile relative to the wind-stress profile for the homogeneous sea surface temperature was obtained when the sea surface temperature was similar to the one for the well-developed upwelling. In the case of the constant sea surface temperature wind-stress profile was fairly constant in the offshore–onshore direction except in the vicinity

* Presented at the Symposium "Observations and Modelling in Geophysics", organized by the Geophysical Institute, Faculty of Science, University of Zagreb. The Symposium was held at Zagreb, Yugoslavia, between 11 and 13 June 1986.

of the coast line. With sea surface temperature profile resembling well-developed upwelling the atmosphere model developed wind-stress profile that had pronounced decrease in 40 km band next to the coast and a weak increase right at the coast.

The ocean model forced with the wind stress obtained from the atmosphere run that had homogenous sea surface temperature, developed strong upwelling zone and quite strong equatorward current with embedded jet near the coast. Forced with the wind stress from the run with nonhomogeneous sea surface temperature, the ocean run had a much weaker upwelling and a double structure of the longshore current with the poleward flow in the vicinity of the coast line and equatorward flow in the region, away from the coast, where wind stress was bigger than the prescribed, vertically integrad y-component of the pressure gradient force.

Priobalna interakcija atmosfere i mora u uslovima izranjanja

Da bi se ispitala mogućnost uzajamne interakcije more-atmosfera u blizini zapadnih obala kontinenata, izvedene su sukcesivne integracije dvodimenzionalnih modela atmosfere i okeana. Atmosferski model ima propisanu temperaturu mora koja se ne menja u toku integracije. Okeanski model je forsiran na osnovu vrednosti za napon vetra.

Oba modela su hidrostatička uz korišćenje Businesk aproksimacije i jedne varijante sigma koordinate, poseduju visoku rezoluciju i u vertikalnom i u horizontalnom pravcu tako da se mogu razložiti i gornji i donji granični sloj. Parameterizacija turbulentnih procesa je urađena u skladu sa tzv. 2.5 nivoom zatvaranja koji su predložili Melor i Jamada. Otvorene bočne granice u oba modela imale su radijacione granične uslove. Okeanski model je imao pripisane vrednosti nivoa mora i y-komponentu pritiska na osnovu osmatranja.

Dnevni ciklus je postignut specificiranjem dnevnog hoda temperature tla dok je noćno hlađenje modelovano njutnovskim forsiranjem. Osnovno stanje u atmosferskom modelu je izvedeno iz osmatranja prikupljenih u CODE-u (Coastal Ocean Dynamics Experiment), dok je vetar na vrhu modela izabran tako da je vrednost napona vetra u blizini mora bliska klimatološkoj vrednosti.

Kada je pripisana temperatura mora bila slična onoj koja se javlja kod dobro razvijenog izranjanja, dobijen napon vetra se značajno razlikovao od onog kada je temperatura mora bila konstantna. U integraciji u kojoj je pripisana temperatura mora bila konstantna profil dobijenog napona vetra je bio približno konstantan, sem u neposrednoj blizini obale. Ako je propisana temperatura mora ličila na profil temperature u slučaju izraženog izranjanja tada je profil napona vetra imao jasno izraženo smanjenje u pojasu 40 km do obale, u odnosu na klimatološke vrednosti koje su dobijene daleko od obale.

Ako je okeanski model forsiran naponom vetra iz integracije atmosferskog modela koji je imao konstantnu temperaturu mora, tada se generiše jasno izraženo izranjanje u priobalnom području uz pojavu struje koja se kreće ka ekvatoru. U neposrednoj blizini obale i u blizini površine pojavljuje se jasno izražen maksimum. Ako je okeanski model forsiran naponom vetra dobijenim iz integracije atmosferskog modela, gde je pripisana temperatura mora bila slična onoj kad postoji izraženo izranjanje, tada je dobijeno izranjanje bilo slabo, dok je struja paralelna s obalom imala pravac k ekvatoru uz obalu i u suprotnom pravcu dalje od obale. Promena znaka toka je bila otprilike tamo gde je napon vetra postajao veći od pripisane y-komponente sile gradijenta pritiska.

1. Introduction

Air-sea interaction has been recognized for a long time as a basic mechanism that can control thermodynamic and dynamic processes either locally or over a large part of the ocean and atmosphere. This paper is concerned with interaction in the vicinity of the land-sea boundary in areas where strong upwelling occurs. Roughly, two distinct air masses with different radiation and heating regimes exist there. Due to the large heat capacity of the ocean, height of the boundary layer over ocean is almost constant during the day. The height of the boundary layer over land, in contrast, is characterized by strong diurnal variations. Another important characteristic of atmosphere in the vicinity of the land-sea boundary is the existence of the transition zone where isotherms slope, near the top of the boundary layer, since most of the time the height of the marine boundary layer is lower than the height of the land boundary layer. Such pattern drives land--sea breeze. The alongshore component of the induced land-sea breeze together with the large-scale, mean wind determines the wind stress that the atmosphere exerts upon the ocean.

Upwelling modifies the local circulation in the atmosphere in comparison with the situation with a homogeneous sea surface temperature. The question is in what direction such modification goes: towards stronger or weaker atmospheric circulations? If the atmospheric circulation gets stronger further upwelling is possible; in other words the air-sea interaction is of a positive feedback nature. The final state will be bounded by dissipation both in the atmosphere and the ocean but would have stronger atmospheric circulation and stronger upwelling relative to the homogeneous sea surface temperature case. Such a possibility was put forward by Clancy, Thompson, Hurlburt and Lee (1979). The crucial parameter is the width of the upwelling zone. In the case of a very narrow upwelling zone, the alongshore component will not be significantly increased even though cross-shore circulation and corresponding vertical velócity may increase. The opposite case of the very broad upwelling zone favors positive feedback, since a significant increase of the alongshore component may be expected. For the intermediate case two competing tendencies are present. First, between the offshore ocean region with warmer sea surface and the upwelling region a pressure gradient force forms that drives near surface winds in the poleward direction (for the western edges of the continents). Ekman transport, due to this component of the wind, reduces upwelling. Second, temperature contrast between the upwelling region and the land surface is increased thus increasing the pressure gradient in that region. This component of the pressure gradient force is driving surface winds towards the equator, favorable for the upwelling. In their paper Clancy et al. conclude :"... althought the sea-breeze affects the upwelling and the upwelling affects the sea-breeze, the air-sea feedback loop to the coastal upwelling is exceedingly weak". This result is understandable since the upwelling zone in their experiments, with a fully coupled air-sea model was only about 8 km wide. There are at least two points in our opinion that leaves the question of the air-sea interaction unsettled after their work. First, their model had relatively poor vertical resolution in both the atmosphere and the ocean part. Second, from the CALCOFI, No 30 atlas (Lynn et al, 1982) the upwelling zone is generally much wider than 8 km.

Whether an atmospheric flow will influence ocean circulation depends strongly on the horizontal, cross-shore derivative of the wind-stress, the wind-stress curl. There is some observational though not conclusive evidence that the wind-stress does have structure within 50 km or less from the coast. If that is the case, then the recent work by Mellor (1986) shows that wind-stress curl will have a significant influence on the upwelling.

Our approach therefore is to examine the response of the atmosphere to the prescribed sea-surface temperature and then the response of the ocean to the wind-stress obtained from the atmosphere model runs. Both models are 2–D, have high resolution in the horizontal and very high resolution in the vertical so that bottom boundary layer in the atmosphere model and both top and bottom boundary layers in the ocean model are resolved.

Special attention was paid to modelling the effects of the large scale motions that are generated by the processes on scales larger than those present in the model. For the atmospheric part we wish to model the diurnal cycle but to avoid expensive radiation calculations. An approximate but efficient way of achieving this is to add Newtonian cooling term to the thermodynamic equation. This term is turned on after 12 hours of heating and should approximate real-world radiation cooling after sunset.

Since we model radiative processes with the Newtonian cooling type term, care was taken in defining the *reference* state to which the model is forced to relax since a large part of the results is determined by the imposed thermal structure. Our main source of data are preliminary results from Coastal Ocean Dynamics Experiment (henceforth, CODE) kindly provided by Dr. K Friehe. The original CODE data are presented in Fig. 1. We have somewhat modified the data, mainly by reducing the slope of the isotherms near the top of the boundary layer in the vicinity of the coast where the marine boundary layer undergoes a transition to land boundary layer. This modification was done in order to make the data compatible with the model resolution and its hydrostatic nature. Similarly, vertical profiles are smoother due to the limitations of the vertical resolution. These are believed to be minor modifications particularly since we view this study as a sensitivity study rather than an attempt to reproduce CODE results. The CODE data were combined with profiles prescribed by Mizzi and Pielke (1983) to fill the region between the top of CODE data (1300 m) and the top of our model (6000 m). The resulting vertical profiles are presented in Fig. 2.

Concerning mean atmospheric winds, we have tried to simulate what is the prevailing pattern for the summer time for the Eastern Pacific near the California coast. The strength of the mean winds was such to give, for the y-component of the wind-stress, values very close to observed climatological values of 0.6 dyn/cm^2.

Both models are for a Boussinesq fluid and the hydrostatic approximation is made. They are formulated in a sigma coordinate system.

The model equations are split into external and internal modes. Separate computations are made for each mode.

Turbulent fluxes and mixing coefficients are parameterized with the so-called 2.5. level, second order closure scheme, proposed by Mellor and Yamada (1974, 1982).

CØDE II PRØFILES FLT 14
DATE 06.02.82 START TIME 24.44.00 END TIME 24.48.24
START LAT= 38.98 LØNG= -124.08 END LAT= 38.79 LØNG= -123.99

CØDE II PRØFILES FLT 14
DATE 06.02.82 START TIME 25.19.42 END TIME 25.24.48
START LAT= 38.63 LØNG= -123.42 END LAT= 38.76 LØNG= -123.55

CØDE II PRØFILES FLT 14
DATE 06.02.82 START TIME 23.12.48 END TIME 23.16.48
START LAT= 38.32 LØNG= -123.07 END LAT= 38.25 LØNG= -123.25

CØDE II PRØFILES FLT 14
DATE 06.02.82 START TIME 23.04.12 END TIME 23.09.30
START LAT= 38.51 LØNG= -122.81 END LAT= 38.37 LØNG= -122.93

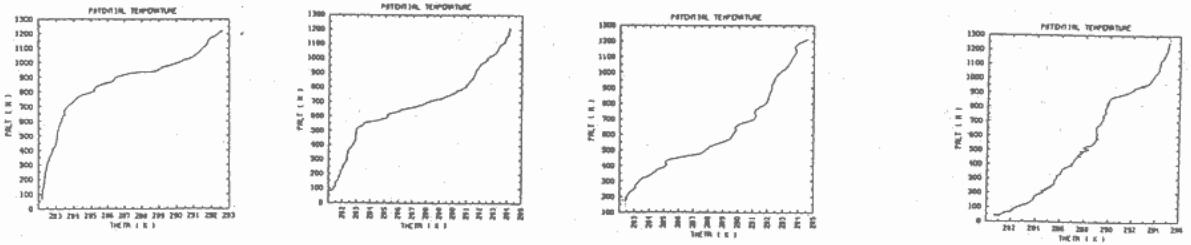

Figure 1 Vertical profiles of potential temperature taken by aircraft during CODE and averaged over flight length. The profiles (a), (b) and (c) are over the ocean while profile (d) is taken over land very near the coast line. Note the consistent reduction of the inversion height of the marine boundary layer as the coast line is approached.

From the modelling standpoint the most difficult problem was the treatment of the side boundaries in the case of nonzero mean flow. The basic approach was to use a form of the radiation boundary condition for the outflow points and to perform one--dimensional calculations with the same turbulent parameterization i.e. omitting only the advection term for the inflow points.

Both the atmosphere and the ocean models have a free surface at the upper boundary. The main reason was to include tidal effects in the ocean model although computational efficiency was increased as well (solving the Poisson equation required by a rigid lid model is bypassed in this way) and it was kept in the atmosphere model.

In mesoscale modelling the diurnal cycle is usually introduced either through specification of the heat flux at the ground or through specification of the time evolution of the temperature at the lowest level of the model. We have chosen the latter method.

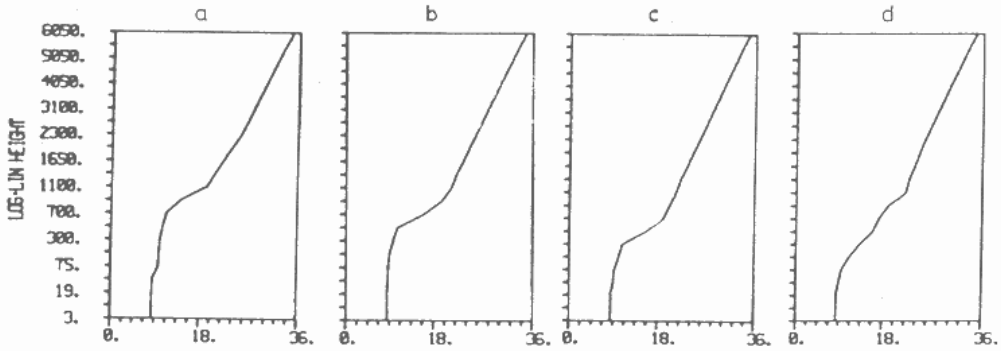

Figure 2. Potential temperature profiles from Fig. 1 smoothed out in vertical consistently with model resolution and extrapolated up to 6 km with temperature gradient as in Mizzi and Pielke (1983). Again profiles (a), (b) and (c) are over the ocean while profile (d) is over land very near the coast line. Note that distribution in z is log+lin.

For all runs, the time evolution of the temperature at the first level over land was prescribed following Mahrer and Pielke (1977), rescaled to the amplitude of the diurnal signal of 12°K at the coast line and increased linearly going inland to 14°K. The ocean surface temperature was kept constant at 8°C throughout all land-sea breeze runs.

Considering the question of the final state of the atmosphere-ocean system with and without upwelling, an interesting question is whether a positive or negative feedback mechanism operates. If inclusion of a nonhomogeneous sea surface temperature causes significant increase in the strength of the atmospheric circulation which in turn causes even stronger upwelling, a positive feedback mechanism operates. Presumably, mutual amplification is ultimately limited by friction but the circulation is stronger than that which had a homogeneous sea surface temperature. If the atmospheric circulation gets weaker with the introduction of a nonhomogenous sea surface temperature, then a negative feedback operates in the atmosphere-ocean system.

We expect that the key parameters are the width and intensity of the imposed upwelling zone. If one starts with a very narrow upwelling zone, then atmospheric adjustment will be mostly through inertial internal-gravity waves that will propagate away without significant change of the atmospheric flows. Also, the time scale on which we may expect changes in the atmospheric winds has to be longer than one day.

Since we wish to determine the coupling between ocean and atmosphere from the consecutive runs of the atmosphere and the ocean model, we should check whether the sea surface temperature imposed on the atmospheric model is consistent with that obtained from the ocean model. First we run the atmosphere model with sea surface temperature prescribed with a thermal gradient. Then we force the ocean with the wind stress from this atmosphere run. The ocean has horizontally uniform tmperature as the initial state. If the sea surface temperature of the resulted upwelling is close to the one that we have prescribed for the atmosphere run, then we have a self-consistent situation. If the imposed and the obtained sea surface temperatures differ, then one should try to infer at least the sign of the response, i.e. does introduction of the upwelling strengthen or weaken atmospehric circulation?

2. Atmospheric circulation near the land-sea boundary

The next series of runs are intended to reveal the relative influences of

– *horizontal temperature gradients in the atmosphere between air mass over land and air mass over sea*

– *nonhomogeneous sea surface temperature on the intensity and structure of the land-sea breeze in the presence of a mean wind.*

To see how each of these parameters influence atmospheric circulation, results are presented in a succession of runs, Fig's 3 to 6. The top panel in these figures shows a reference state for a particular case. The next panel presents imposed sea surface temperatures. The third panel presents potential temperature fields at 12:00, from the fourth day of integration, and the bottom panel is the 24 hours average, from the last day of integration, of the calculated wind stress. Note the change of the scale of the abscissa for the wind stress distribution. The temperature fields are for the whole atmospheric domain of 500 km (from $x_L = -250$ km to $x_R = 250$ km). The wind stress profile distribution is only over the oceanic portion of the domain, from $x = -80$ km to $x = 0$.

CASE A. The reference state for case A is presented in Fig. 3 (a). It is horizontally homogeneous with homogeneous temperature of 8°C at the lower boundary over the ocanic part of the domain, close to the values for the sea surface temperature from the CODE data. The alongshore wind component is enhanced by the diurnal cycle. During most of the day, the land region is warmer with lower pressure relative to the pressure over the ocean. Such pressure distribution drives the alongshore wind component in the equatorward direction which is the same direction as the V-component of the imposed mean wind.

From the shape of the wind stress distribution (d) we can estimate that diurnal forcing affects the ocean in a band approximately 20 km wide next to the coast. Imposed geostrophic wind produces a uniform stress of about 0.6 dyn/cm^2.

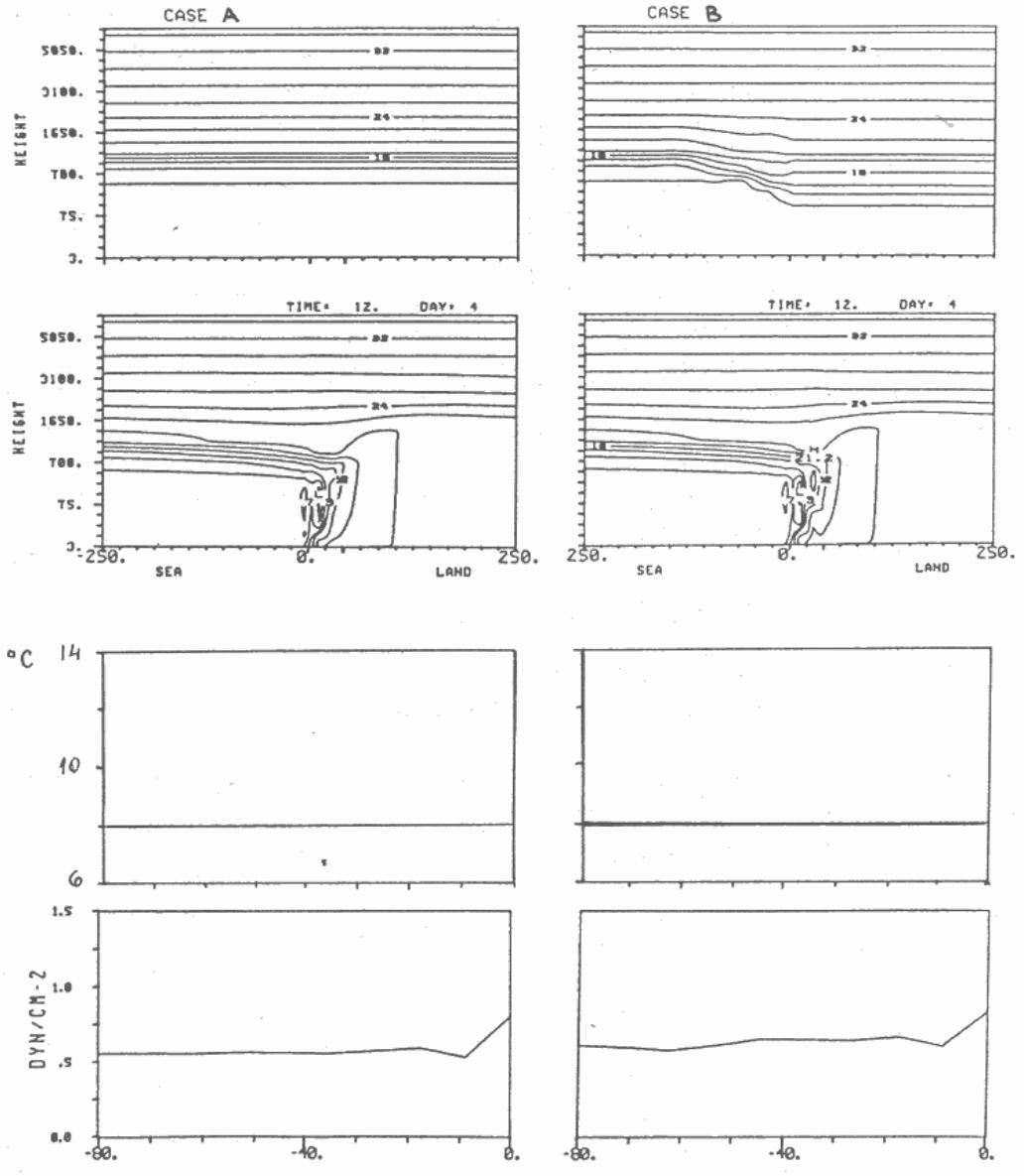

Figure 3. (a) – case A with horizontally homogeneous potential temperature reference state. Sea surface temperature constant, 8°C. Case B with horizontally nonhomogeneous potential temperature reference state. Sea surface temperature constant, 8°C.

(b) – imposed sea surface temperature distribution.

(c) – potential temperature fields at 12:00, from the fourth day of atmosphere model integration.

(d) – wind stress profiles from the 80 km band averaged over fourth day of the atmosphere model integration.

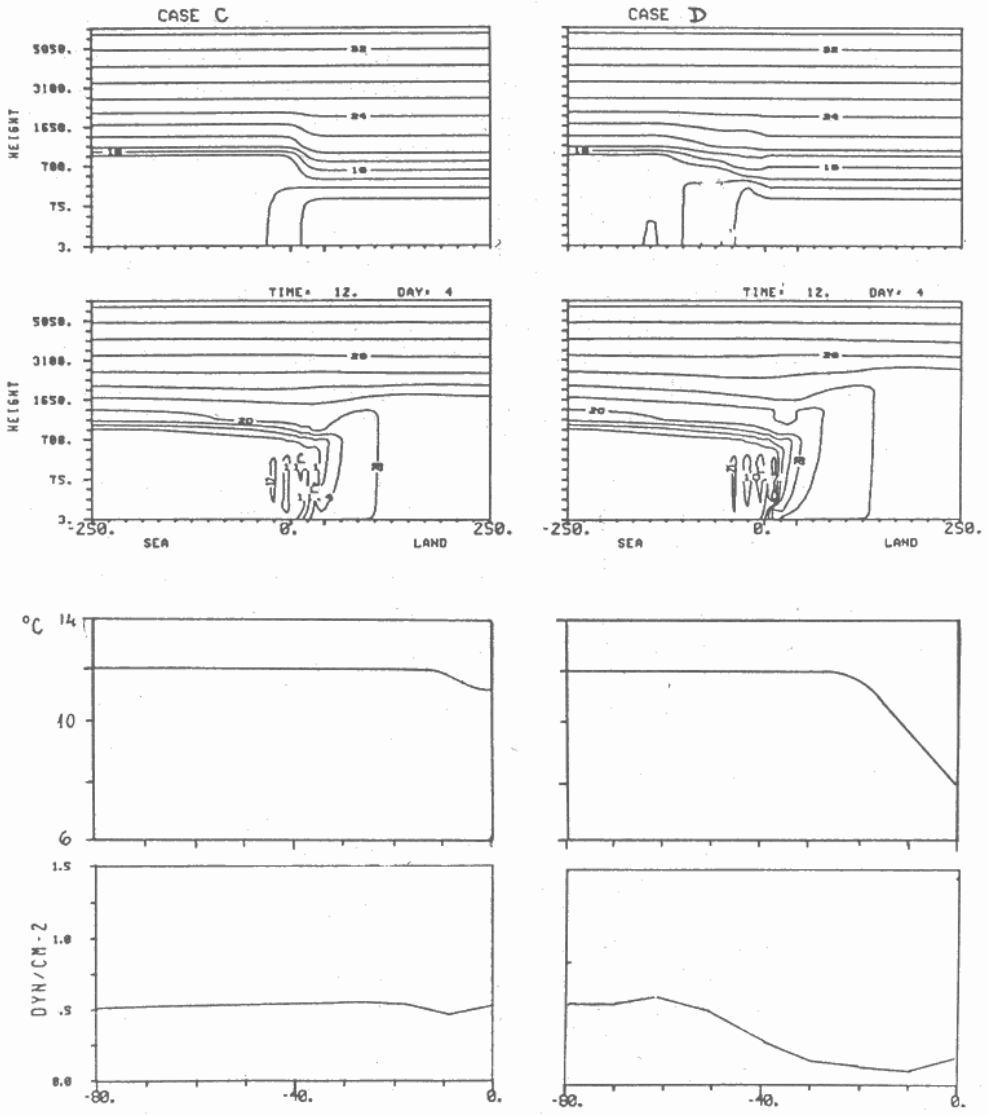

Figure 4. (a) – case C with horizontally nonhomogeneous potential temperature reference state with constant sea surface temperature equal 12°C. Case D with horizontally nonhomogeneous potential temperature reference state.

(b) – the imposed sea surface temperature distribution.

(c) – potential temperature fields at 12:00, from the fourth day of atmosphere model integration.

(d) – wind stress profiles from the 80 km band averaged over fourth day of the atmosphere model integration.

CASE B. In case B a horizontal temperature gradient has been introduced in the reference state. The temperature at the lower boundary over the oceanic part of the domain is the same as in case A, 8°C. Temperature fields (c) for cases A and B look quite similar. However, a comparison of the time averaged wind stress distribution reveals that case B develops a stronger wind stress, indicating a somewhatt stronger, local circulation.

CASE C and **CASE D.** Case D represents a further modification in the direction of the realistic reference temperature field through introduction of a new temperature distribution at the lower boundary, over the oceanic part of the domain. Since temperature at the lower boundary is 12°C, except near the coast, the corresponding homogeneous oceanic temperature case is the one with 12°C. Comparison between cases C and D shows the influence of the nonhomogeneous sea surface temperature on the structure of the wind stress. The land surface temperature in the reference state is the same for both cases, 8°C.

The main characteristic of case D is a pronounced drop in the wind stress in the region 10–60 km's away from the coast. The position of the minimum in the wind stress coincides with the position of the minimum in the temperature at the lower boundary. Geostrophic balance then requires that to the left of the temperature minimum V-component is driven in the poleward direction, opposing V-component of the mean wind. On the other side of the temperature minimum, the pressure gradient force acts in the same direction as the mean pressure gradient force. Case *C* has a transition region also but of the order of 10 km, too short to influence the alongshore component. It does influence the wind and wind stress profile next to the land-sea boundary and that seems to account for the differences between cases A and C in that region.

CASE E. Since the width of the observed upwelling zone is quite variable along the coast, the next case has again nonhomogeneous sea surface temperature. Case E shows what happens if the upwelling zone doubles (note that due to the assumption that boundary layer is well mixed below the inversion layer, that implies a broader transition zone in the atmosphere boundary layer as well). Modification of the wind stress profile relative to the homogeneous sea surface temperature case is much stronger and occurs over the whole 80 km ocean domain. Further away wind-stress gains values that are close to observed climatological values.

CASE F and **CASE G.** What happens to the comparison of the atmosphere response to the homogeneous versus nonhomogeneous sea surface temperature if the land temperature is 12°C, higher by 4°C than in the previous cases? The answer to that is in cases F and G presented in Fig. 6. Since the portion of the reference temperature field above the inversion layer remained unchanged, the main characteristic of the cases is the reduced inversion layer strength. That gave an increase of the circulation strength and consequently increase in the wind stress, although in qualitative sense the situation is the same as in pair A and D.

The basic conclusion from all runs is that the width of the upwelling zone is a dominant parameter in shaping of the wind stress profile. It induces a strong minimum in the wind-stress profile in the region of upwelling. Such behavior is completely absent in

all cases with a homogeneous sea surface temperature. The second factor is the strength of the inversion layer. It influences the strength of the wind-stress. The influence is nonlocal, it spreads over the whole domain.

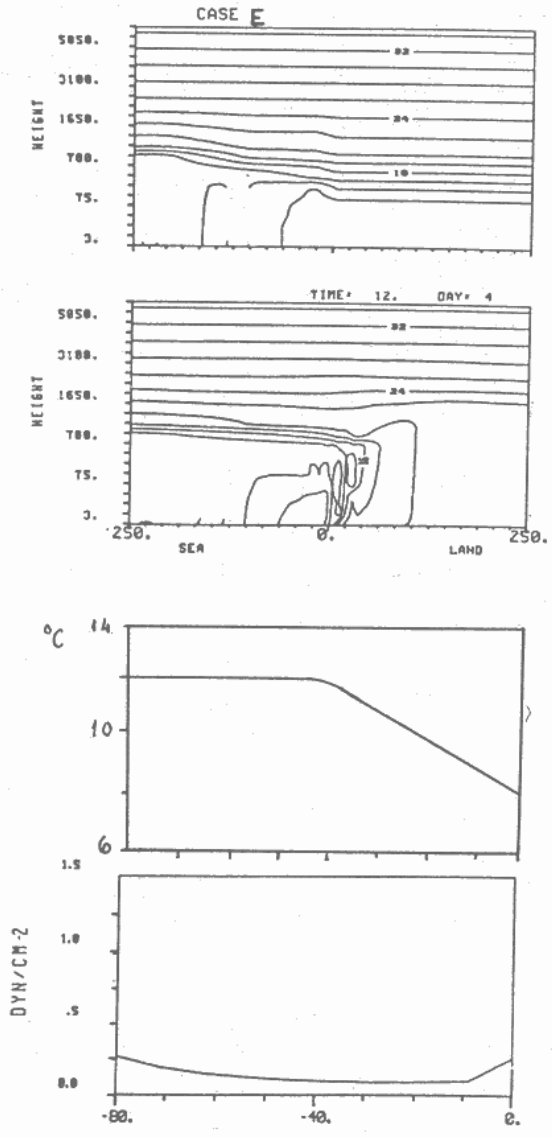

Figure 5. Same as in Fig. 3 except for case E where sea surface temperature distribution has transition zone of 40 km.

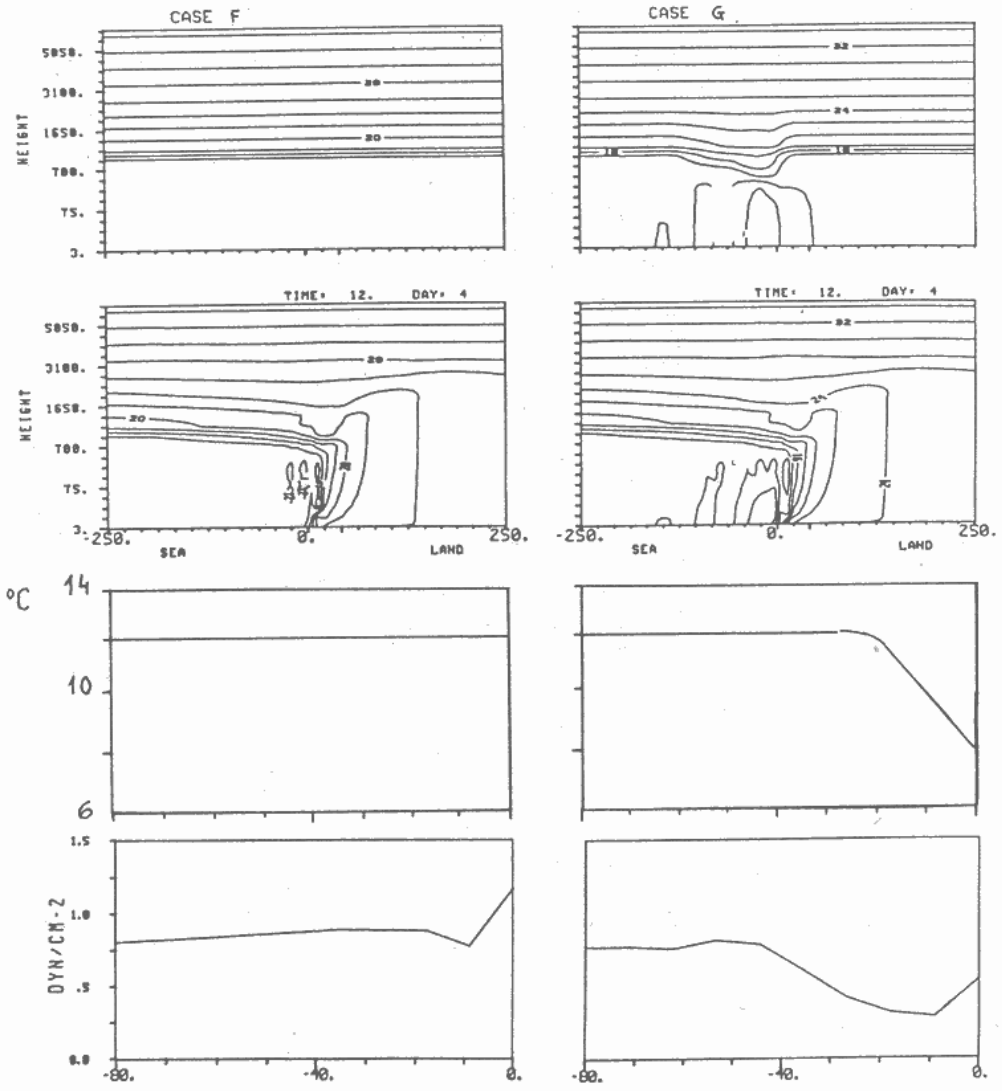

Figure 6 Same as in Fig. 3 except for case F the sea surface temperature is homogeneous and is 12°C. For case G sea surface temperature is nonhomogeneous while the land surface temperature in the reference state is 12°.

3. Ocean response to the atmosperic forcing and coastal upwelling

3.1 Some observational facts and preliminary discussion

When wind with a nonzero wind stress curl blows over the ocean, upwelling or downwelling is induced. Upwelling if the wind stress curl is positive, downwelling if the wind stress curl is negative. In the coastal regions of the ocean it is sufficient that wind

has a component parallel to the coast line. The presence of the sloping topography is an additional contributor to upwelling or downwelling flow structure. Beside these geometrical factors, the structure of the alongshore current plays an important role in the occurrence of the upwelling or downwelling.

We are concerned only with the generation of upwelling or downwelling by the local forcing i.e. we assume that wind stress is uniform along the coast. In the model the coast line is in the south-north direction.

Following the work of Mellor (1986) we examine the longtime averaged and alongshore averaged flow structure. Then, starting with the equations of motion one can obtain a balance that is relevant for the long time averages (we neglect nonlinear terms)

$$-fV = -gH\partial_x\eta - \int_{-H}^{0}\int_{-H}^{0} \partial_x b\,dz\,dz + 0 - \tau_x{}^b \tag{1},$$

$$\int_{-H}^{0} u\,dz = 0 = -\frac{gH}{f}\partial_y\eta - \frac{1}{f}\int_{-H}^{0}\int_{-H}^{0} \partial_y b\,dz\,dz + \frac{\tau_y^0}{f} - \frac{\tau_y{}^b}{f} \tag{2},$$

(A) (B) (C) (D)

where b is buoyancy and is defined as $b=g\rho/\rho_0$, τ is wind stress, η is sea surface elevation, H is depth and the rest of the symbols have the usual meaning.

So, for a steady state, balance must exist between onshore–offshore pressure gradient force (sum of A and B) Ekman surface transport (term C) and bottom Ekman transport (term D). Since term C represents the origin (driving) of the upwelling it is called an index of upwelling.

The y-component of the pressure gradient is prescibed from Mellor (1986), based on the observations Bakun (1978). Mellor also estimates from Nelson and Hussby (1976) that the spatial and temporal average for τ_y^0 is about 0.6 dyns/cm^2.

Since equations (1) and (2) represent a balance valid for the steady state, we can regard the state that they describe as an end of adjustment of the ocean flows to the wind or thermal forcing. We can think about the adjustment process to the wind forcing in terms of two modes, barotropic and baroclinic. The wind stress induces Ekman transport away from the coast and a dip in the surface elevation develops, thuy $\eta_x > 0$. The change of elevation will produce a u-acceleration. That, through the Coriolis term will accelerate the v-component and, in the end, a steady state will be reached with a balance between the Coriolis term and pressure gradient force, $g\eta_x$ that a surface current flows in the same direction as the surface wind (in our case, equatorward). This part of the response is the barotropic response (mode). Linear theory estimates the length scale of this mode to be roughly $\sqrt{gH_0}/f \sim 200$ km. Near the surface and the bottom, the geostrophic relation is strongly modified by the respective boundary layers. Very near the coast the effective windstress profile is a step function which drives upwelling.

Mellor (1986) discusses the influence of the shape of the wind stress alone on the structure of the coastal flows and upwelling. He examined three idealised profiles that are presented in Fig. 7.

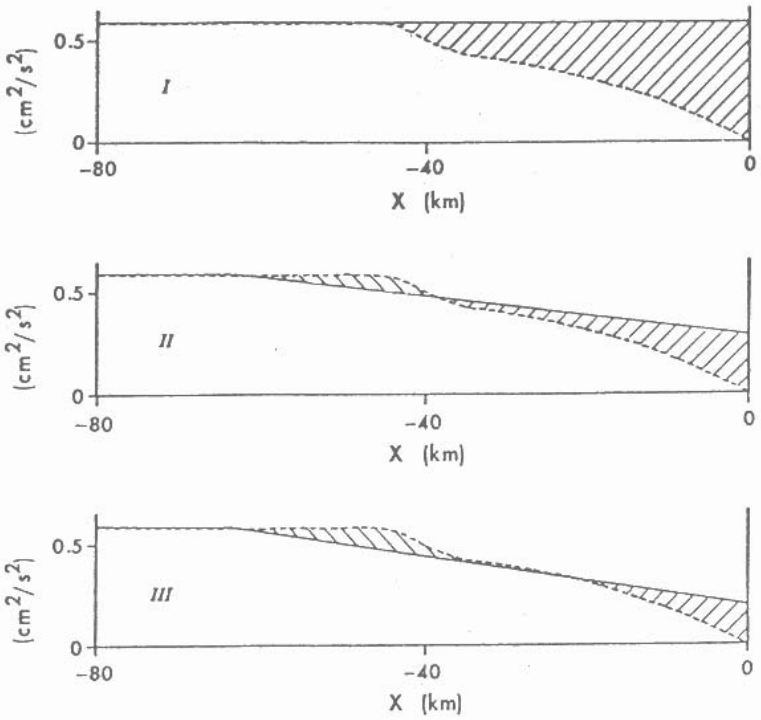

Figure 7 Wind stress distributions (solid curves) with different curls and integrated alongshore pressure gradients (dashed curves) are defined in this plot. The bottom stress, $\tau_y{}^b$, is the vertical integral of the cross hatched area: /// is positive corresponding to upwelling bottom boundary transport; \\\ is negataive corresponding to downwelling transport.

The response of the coastal part of the ocean is different for each of the three profiles, Fig. 8. The case, with a constant value for τ_y^b shows upwelling, well-developed surface boundary layer and weaker bottom boundary. The flow is in equatorward direction with maximum at the surface. In the second case, a weak undercurrent is developed while the upwelling is weaker than in the first case. The last case has undercurrent that has surfaced and is quite strong with maximum of 5 cm/s, while upwelling is even weaker than in the second case.

These runs, even though with highly idealised wind stress profiles, are clear examples of the transition from a regime where we have only equatorward surface currents to cases where poleward current develops and gains considerable strength.

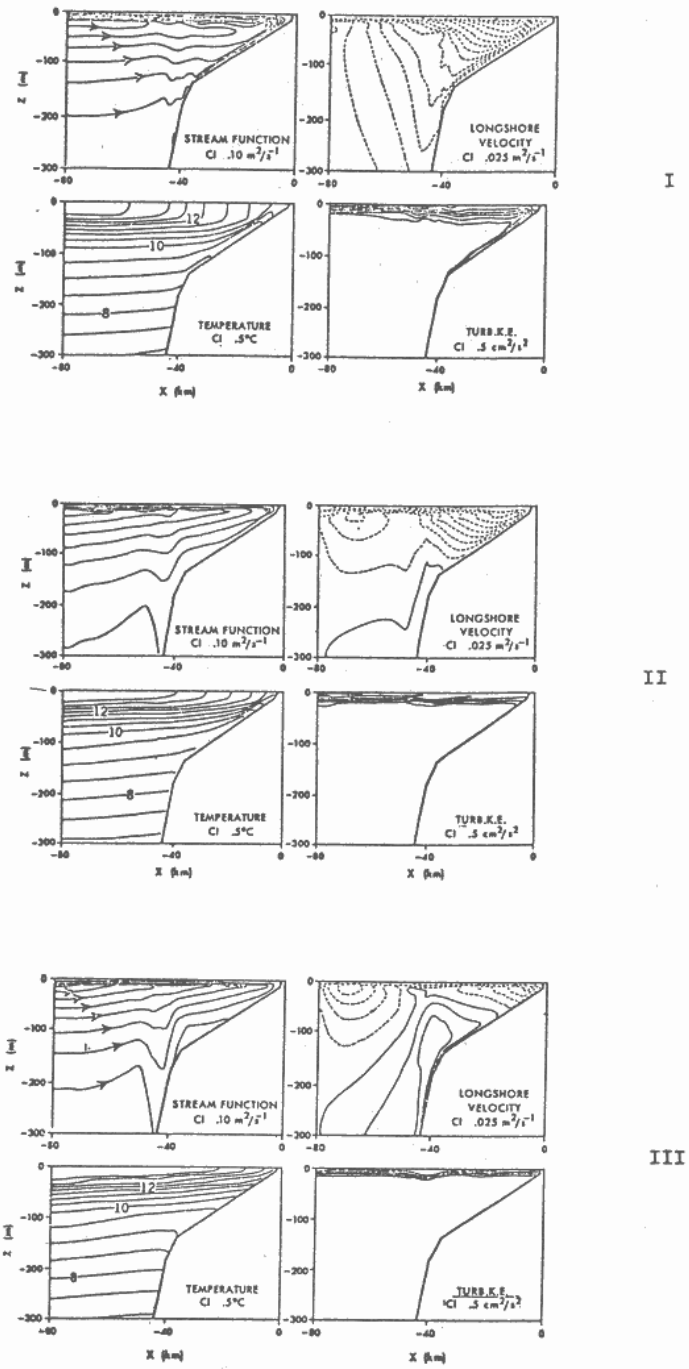

Figure 8 Response of the model ocean to the three types of the wind stress distributions from Fig. 7, after 60 days of integration, from Mellor (1986).

3.2. The analysis of the model runs

In Fig's 9 and 10 are presented our ocean model runs, in relevant pairs that had forcing from the corresponding pair of atmospheric model runs (A, B, C and D). The top panels present 24 hours' means of the calculated wind-stress (full line) and the prescribed integrated y-component of the pressure gradient (dashed line). The middle two panels are calculated potential temperature fields after 40 days of integration. The bottom panels present alongshore flow structure after 40 days of integration with full lines for poleward direction and dashed lines for the equatorward direction. The cases are labeled as case IV, V, VI and VII following the Mellor cases I, II, III.

Cases IV, V. Cases IV and V presented in Fig. 9, have forcing from the atmospheric runs A and B, repectively. The main features of case IV are that flow above 250 meters

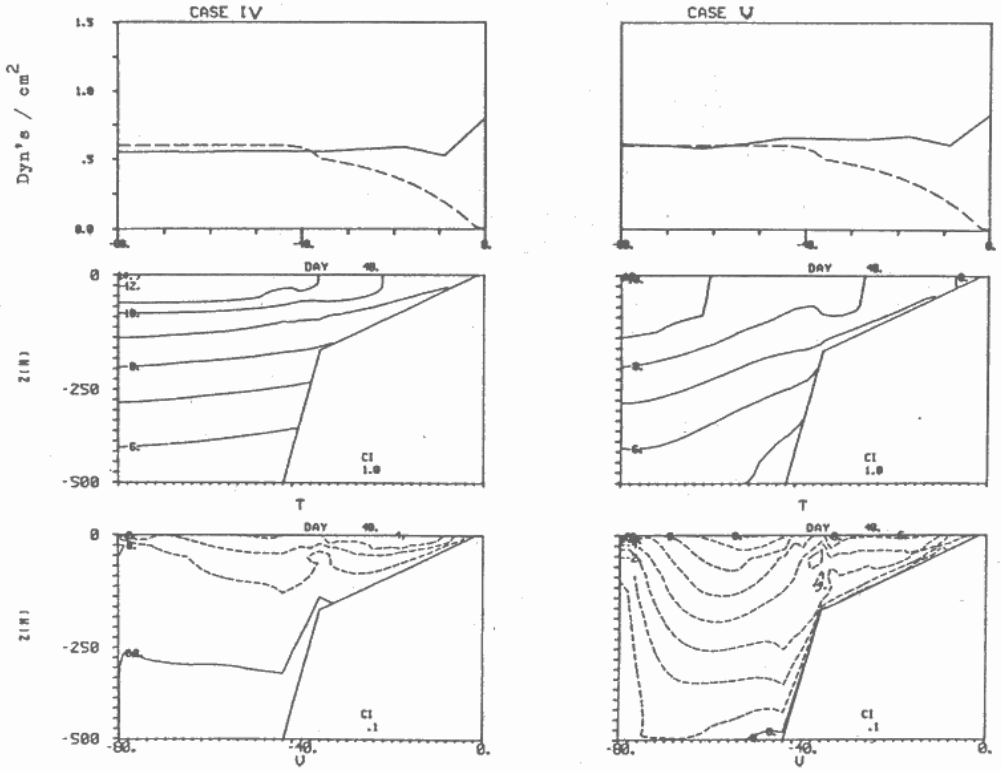

Figure 9 Response of the model ocean to the wind stress distribution obtained with the atmosphere model. Cases IV and V correspond to the cases A and B of the atmosphere runs from Fig. 3.

(a) – wind stress distribution, full line and integrated pressure gradient force prescribed from the available data, dashed line.

(b) – potential temperature fields for the day=40.

(c) – alongshore component of the velocity from the same period. Dashed lines designate equatorward flow, full lines designate poleward flow.

is equatorward while below it a weak poleward current exists. The separation point is where wind stress gets bigger than the integrated pressure gradient. Sloping of the zero line is presumably induced by the sloping of the shelf. Since in the region near the coast wind stress is stronger than the imposed pressure gradient, an intense equatorward current forms and quite intense upwelling occurs. Both surface and bottom boundary layers are well developed. Case V has only an equatorward flow and it is stronger than in case IV. Upwelling is stronger with almost 2 degrees colder surface waters next to the coast. Therefore a conclusion from these two runs is that ocean response is stronger if it is forced by the atmospheric model that has nonhomogeneous thermodynamic state. In both runs the flow structure is similar to the flow structure for case I of Mellor (1986).

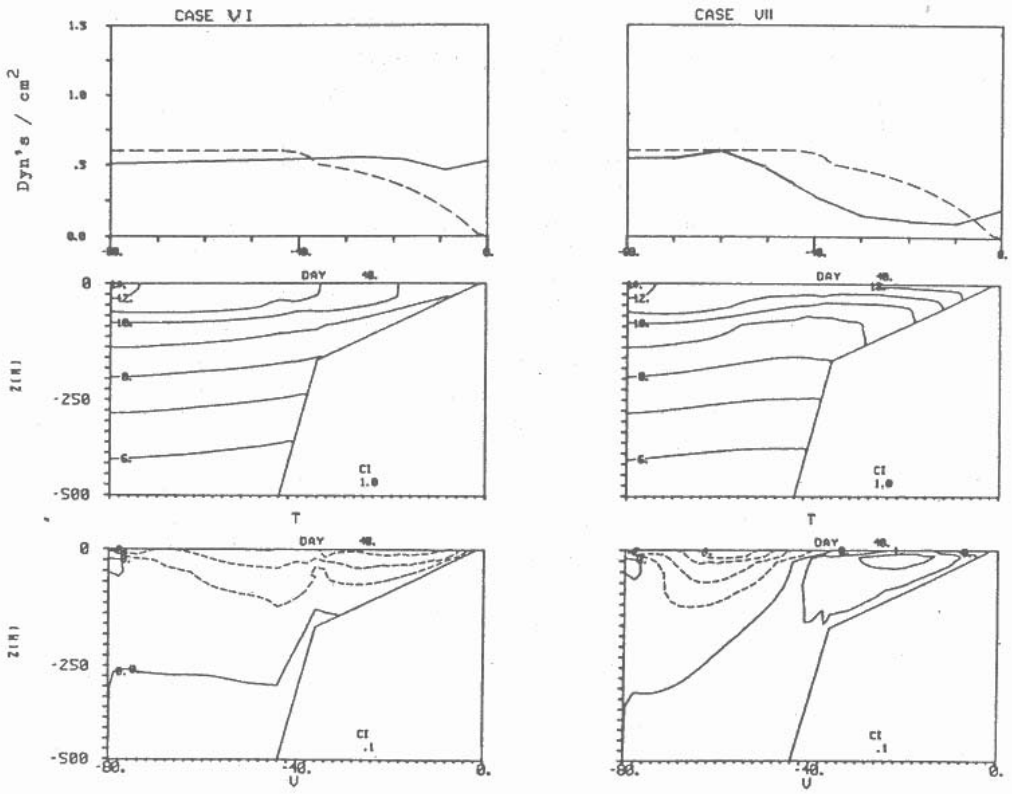

Figure 10 Same as in Fig. 9 except that cases VI and VII correspond to the cases C and D of the atmosphere runs from Fig. 4.

Since in both runs upwelling was developed, the resultant sea surface temperature differs from the imposed, homogeneous sea surface temperature in the atmospheric cases A and B. Thus the atmosphere and developed ocean states are inconsistent in that sense. Therefore, the next step is the run that represents ocean response to the forcing from the atmosphere run that had a nonhomogeneous sea surface temperature. That is case D. Since its sea surface temperature at the open boundary is about 12°C, that was the value

for the sea surface temperature prescribed for the corresponding homogeneous sea surface temperature atmospheric run, case C. The ocean run that has forcing produced in case C is labeled VI. The run that corresponds to the atmospheric case D (nonhomogeneous sea surface temperature) is labeled VII.

Cases VI and VII. Results from case VII are presented in Fig. 10. Relation between the calculated wind stress and the imposed integrated pressure gradient is very different in this case from the previous ones resulting in a quite different flow structure. The main characteristic is a double structure of the alongshore flow. Nearshore region now has a poleward flow with an embedded coastal jet. Beyond the point where wind stress becomes equal to the pressure gradient the flow becomes equatorward. Upwelling is much weaker compared to case V or VI. Case VII has surface waters 4°C warmer than in case V, almost homogeneous over the region with a weak temperature gradient of the opposite sign in the region over poleward flow. That feature is not present in the imposed sea surface temperature profile. Case VI shows an ocean response very similar to that of case IV since the wind stress profiles for the two runs are very similar.

The qualitative change of the ocean flows from case VI to case VII shows that reduction of the wind stress seaward from the local temperature minimum is much stronger effect than increase of the land-sea temperature contrast very near the land-sea boundary.

Having in mind results from cases IV, V, VI and VII and results from the atmospheric cases C and D we can construct a spin up scenario for a coupled ocean-atmosphere model in two phases. First, we start with a homogeneous sea surface temperature and prescribed mean winds. After several diurnal cycles a wind-stress distribution will be produced like the one in the atmospheric case C. That will start forcing of the ocean towards state similar to the oceanic case VI. Changed sea surface temperature will cause change of the wind-stress distribution becoming similar to the one of the atmospheric case D. When the wind stress gets smaller then the vertically integrated pressure gradient change of the flow structure occurs and further upwelling stops.

References

Bakun, A., (1978): Coastal Upwelling off Western North America, 1975. NOAA Technical Report NMFS Circular 416–, 89–103.

Clancy, R.M., J.D. Thompson and H. E. Hurlburt (1979): A model of mesoscale air-sea interaction in a sea breeze-coastal upwelling region. Monthly Weather Review **107**, 1476–1505.

Lynn, R. L., K. A. Bliss and L. E. Eber, (1982): Vertical and horizontal distribution of seasonal mean temperatures, salinity, sigma-t, stability, dynamic height, oxygen saturation in the California Current, 1950–1978. CALCOFI Atlas No. 30, Marine Life Research Program, Scripps Institution of Oceanography, La Jolla, CA.

Mahrer, V. and Pielke, R. A. (1977): The effects of topography on the sea and land breezes in a two-dimensional numerical model. Monthly Weather Review **105**, 1151–1162.

Mellor, G. L., (1986): The numerical simulation and analysis of coastal ocean circulation of California. Continental Shelf Research, **6**, 689–713.

Mellor, G. L., and T. Yamada, (1982): Development of a turbulence closure for geophysical problems. Reviews of Geophysics and Space Physics, **20**, 851–875.

Mizzi, A. P., and Pielke, R. A. (1983): A numerical study of the mesoscale atmospheric circulation observed during a coastal upwelling event on August 23, 1972. Part I: Sensitivity studeis. Monthly Weather Review, **112**, 76–90.

Nelson, C. S., and D. M. Hussby, (1976): Climatology of Surface Heat Fluxes over the California Current Region., 156pp,. NOAA Technical Report, NMFS SSRF-763, 155pp, National Oceanic and Atmosphere Administration, Washington, D. C.

Yamada T. and Mellor, G. L., (1974): A hierarchy of turbulence closure models for planetary boundary layers. Journal of Atmospheric Sciences, **31**, 1791–1806. (corrigenda, Journal of Atmospheric Sciences, **34**, 1482.)